Hindawi Publishing Corporation
Advances in Materials Science and Engineering
Volume 2016, Article ID 5753970, 8 pages
http://dx.doi.org/10.1155/2016/5753970

Research Article

Synergism Analysis of Bedding Slope with Piles and Anchor Cable Support under Sine Wave Vehicle Load

Li Dan-Feng and Wang Lian-Jun

School of Civil Engineering, Beijing Jiaotong University, Beijing 100044, China

Correspondence should be addressed to Li Dan-Feng; lidanfeng1903@163.com

Received 25 April 2016; Revised 24 July 2016; Accepted 7 August 2016

Academic Editor: Hossein Moayedi

Slope instability under dynamic load is the technical difficulty in the engineering; the evaluation of slope stability under dynamic load and the control of dynamic load is particularly important. In this paper, taking the right side slope of K27+140 m~380 m typical section (K27 slope for short) in Chongqing Fuling-Fengdu-Shizhu expresses highway as an example to calculate and analyze. The K27 slope is under sinusoidal vehicle load and supported by anchor cable and antislide pile to resist downslide strength; at the same time, the combined effect of them is studied. Three-dimensional finite element methodology (FEM) is used to simulate the bedding slope with piles and anchor cable support; furthermore, the eigenvalue can be obtained. In order to reduce error of the elastic boundary conditions caused by the reflection effect of wavelengths, the combination of Lysmer surface viscous boundary and traditional ground support boundaries is utilized to analyze and calculate the time-histories during bedding slope under dynamic load. The dynamic response of pile anchor support to resist sliding force is obtained. The concept of the pile anchor supporting coordinate interval is put forward. Furthermore, it is verified that the pile anchor supporting coordinate interval can be used to evaluate the stability of the slope under dynamic load and provide a new method for the control of the dynamic load.

1. Introduction

Anchor pile support has been widely used in slope engineering. Regarding vehicle dynamic load, methods of slope stability evaluation with the pile anchor supporting are not diverse. According to the situation of horizontal seismic, the improvement, using vertical and horizontal bar points to keep slope stability analysis, is analyzed by Dong and Zhu [1]. Le et al. [2] use the software, ABAQUS, to simulate and analyze the stability of foundation pit supporting structure system under traffic dynamic load, drawing the conclusion that horizontal displacement of retaining piles and the changing rule of the axial force of anchor bolt accords well with the numeric simulation results. Using upper-bound theorem of limit analysis, Luo et al. [3] set reinforced slope anchor pile composite structures as an example to derive the resistance and yielding acceleration formulas of slop reinforced by anchor pile. Meanwhile, forecasting methods are put forward, offering the theoretical basis of slop structure design at seismic belt. Guo et al. [4] analyze the influencing factors of excavation influential surface and excavation earth pressure and obtain the required resistance to keep the soil mass stable. Afterwards, the specific methods of calculating the axial force of soil nail at the excavation stage are raised, and the methods are appropriate for the calculation of anchor axial force. Zhu et al. [5] analyze the dynamic response of stable silt subgrade under traffic load, getting the result of subgrade deformation law. Fang et al. [6] utilize the finite element method to compare the pile to strengthen slope only to pile anchor composite reinforcement one, getting the load from upper side slope after being reinforced, hereby evaluating slope reinforcement effect. According to the above, the researches on slope supported by anchor pile under dynamic load are divided in two kinds: one is the improvement of the calculation of the slope stability; the other is the analysis and estimation to the specific slope supported by anchor pile under specific load. However, the synergism analysis and estimation to slope supported by anchor pile are imperfect. Therefore, based on the former research, the stability of slope is analyzed from the perspective of anchor pile supporting synergism.

For the right side slope of K27+140~27+380 typical section (K27 slope) in Chongqing Fuling-Fengdu-Shizhu

Table 1: Lithology and supporting structure calculation parameters.

Lithology and supporting structure	Elasticity modulus Mpa	Poisson's ratio	Appearance density kN/m^3	Cohesion kN/m^2	Friction angle/deg
Intermediate weathered sandstone	4609	0.17	25.18	1793	35.4
Intermediate weathered silty mudstone	2306	0.29	25.71	1056	34.3
Strong weathered silty mudstone	25	0.25	20	12.5	12.05
Slide-resistant pile	250000	0.2	24	—	—
Anchor	195000	0.3	78.5	—	—
Frame beam	10000	0.2	21	—	—

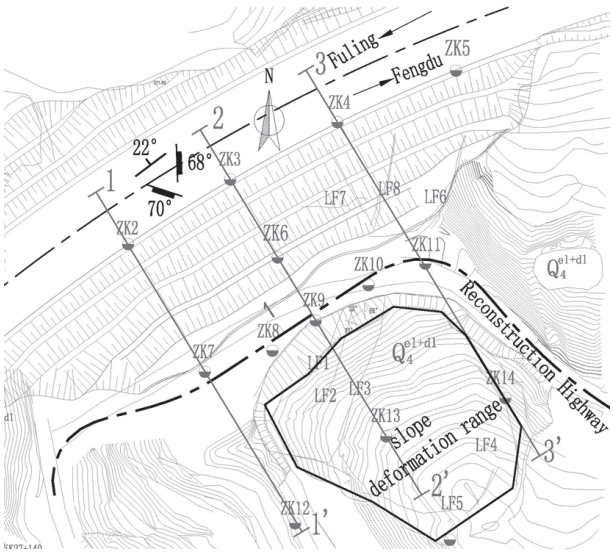

Figure 1: Planar graph of K27 slope.

express highway, the height is 34 m, the length is 160 m, and the average thickness of potential sliding slope is about 18 m, the area is about 10000 m^2, and the body volume is about 1872 m^3. The bedding slope supported by anchor pile on the highway, Chongqing section of K27+140~27+380, is conducted by the free vibration analysis, to reach the dynamic characteristics, using which to analyze dynamic response of the combination of anchor cable with frame beam and antislide pile under sine wave load. Putting forward the supporting coordinate interval could help to estimate the effect of anchor pile supporting. Finally, combined with the monitored field data, the conclusion drew that the supporting coordinate interval can estimate the effect of anchor pile supporting well and provide the theoretical estimation foundation to slope with anchor pile supporting under dynamic load. Planar and sectional drawings of K27 slope are shown in Figures 1 and 2.

2. Engineering Features and Models

2.1. Model Size and Parameters. The slope on right side of express highway at Chongqing section of K27+140~27+380 is simulated, and the maximum slope height is 34 m; length of slope is 160 m. The slope is excavated with five-grade platform of slope, and classified slope height is 8 m. The first and second step of slope rate are 1 : 1, the third and fourth step of slope rate are 1 : 1.5, and the fifth is 1 : 1.25. Local road after renovation goes at the parallel extended routes of slope crest with the antiskating way of anchor-frame-pile combination, which is to set up slide-resistant pile with the length of 20 m at the second stage. The third step laid two rows of anchor cable with the length of 20 m, differently at anchor cable section of 10 m. The bottom-up lithology is intermediate weathered sandstone, intermediate weathering silty mudstone, and strongly weathering silty mudstone. The section size and supporting structure parameters are listed in Figure 3 and Table 1.

2.2. FEM 3D Numerical Model. The numerical model is established according to the actual size. Considering that calculating intact model is complicated, therefore a typical section is chosen from the whole slope, using the Mohr-Coulomb yield criterion. Stratum is set to solid element; in addition slide-resistant pile and framed girder are set to beam element. Implantable girder is used to build the anchor cable [7–9]. FEM 3D numerical model diagram is shown in Figure 4.

3. Free Vibration Characteristics of K27 Slope

Free vibration means eigenvalue analysis; primarily, the inherent dynamical eigenvalue is gotten from the model, meanwhile obtaining the dynamic characteristics, such as natural period of structure vibration, mode of vibration, and participation coefficient. When applying dynamic finite element method to slope model, infinite field needs to turn to finite field, which means that one simulated section should be separated from the whole geologic body, adding boundary conditions to it and then establishing dynamic analysis equation to solve the dynamics problem with structural dynamics and method [9–13]. The model eigenvalue is computed through setting elastic boundary.

Curved surface spring is used to define the elastic boundary needed when calculating the reaction coefficient, which is computed as the equation listed as follows:

Coefficient of horizontal subgrade reaction:

$$k_s = k_{s0} \cdot \left(\frac{P_s}{30}\right)^{-0.75}. \quad (1)$$

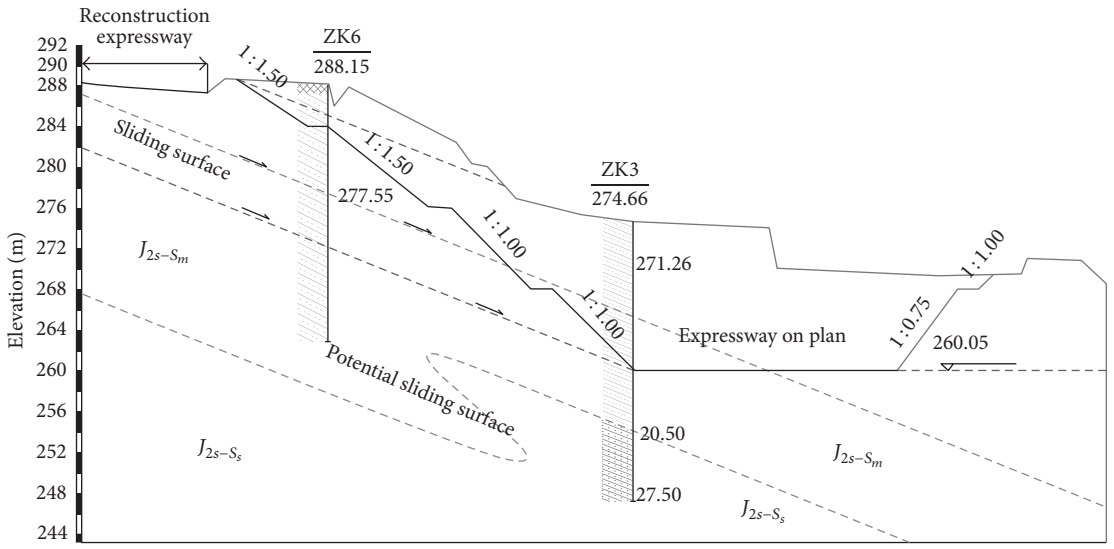

Figure 2: Sectional drawings of K27 slope.

Table 2: Foundation reaction coefficient of every stratum.

Lithology	Intermediate weathered sandstone kN/m^3	Intermediate weathered silty mudstone kN/m^3	Strong weathered silty mudstone kN/m^3
Horizontal	133998	137196	—
Vertical	225577	98332/137199	3449
Normal	215823	78628	1722

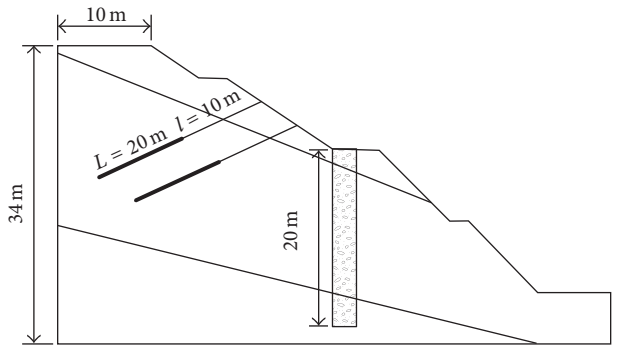

L: length of the anchor
l: length of the anchoring section

Figure 3: Slope design cross-sectional size graph.

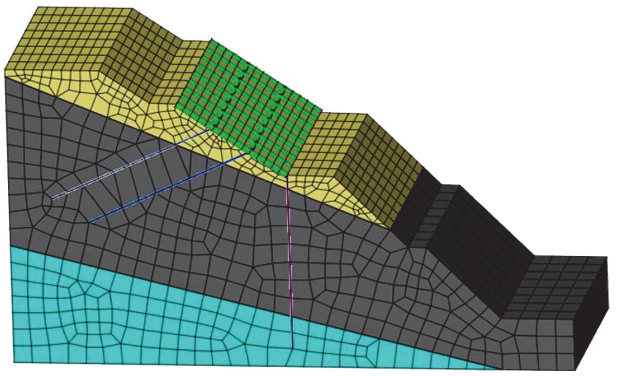

Figure 4: FEM 3D numerical model.

Coefficient of vertical subgrade reaction:

$$k_h = k_{h0} \cdot \left(\frac{P_h}{30}\right)^{-0.75}. \quad (2)$$

In the formulas, $k_{s0} = k_{h0} = \alpha E/30$, $P_s = \sqrt{A_s}$, $P_h = \sqrt{A_h}$; A_s and A_h are sectional stratum areas at horizontal and vertical direction, respectively; E is the subgrade elastic modulus; the value of α is 1.0 as usual. According to the above, the modulus of subgrade reaction is obtained in Table 2.

In accordance with the parameters, the eigenvalue comes out in Table 3.

4. Time-Histories Analysis of Bedding Slope with Anchor Pile Supporting

Under the dynamic load, analyzing the time-histories could help get the slope displacement and internal force at any moment. The dynamical equilibrium equation is as follows:

$$[M] \cdot u''(t) + [F] \cdot u'(t) + [P] \cdot u(t) = T(t). \quad (3)$$

Table 3: Eigenvalue analysis results of slope.

Mode of vibration	Frequency		Period
	rad/s	r/s	s
1	25.917812	4.124948	0.242427
2	28.374287	4.515908	0.221439
3	28.891378	4.598206	0.217476
4	29.356005	4.672153	0.214034
5	30.048622	4.782387	0.209101
6	30.790098	4.900396	0.204065
7	31.660923	5.038992	0.198452
8	33.342720	5.306659	0.188442
9	34.083767	5.424600	0.184345
10	34.865822	5.549068	0.180210

In the formulas, $[M]$ is mass matrix; $[F]$ is damping matrix; $[P]$ is stiffness matrix; $T(t)$ is dynamic loading; u'' is relative displacement; $u'(t)$ is velocity; $u(t)$ is acceleration.

For the reason that errors induced by wave reflection would not be neglected at elastic boundary, therefore surface viscous boundary, proposed by Wang [14], is utilized to analyze the dynamic time-histories. At the same time, combining it with conventional ground reaction boundary will make the model more reasonable [15].

4.1. Damping Value at Viscous Boundary. In order to define the viscous boundary, the damping ratio of slope model ought to be figured out at horizontal, vertical, and normal direction. Equations to calculate the damping ratio are classified as P wave (pressure wave) and S wave (shear wave) as follows:

P wave:

$$C_{\mathrm{P}} = \rho \cdot A \cdot \sqrt{\frac{\lambda + 2G}{\rho}} = \gamma \cdot A \cdot \sqrt{\frac{\lambda + 2G}{\gamma \cdot 9.81}} = c_p \cdot A \quad (4)$$

S wave:

$$C_{\mathrm{S}} = \rho \cdot A \cdot \sqrt{\frac{G}{\rho}} = \gamma \cdot A \cdot \sqrt{\frac{G}{\gamma \cdot 9.81}} = c_s \cdot A. \quad (5)$$

In the formulas, λ is volumetric modulus of elasticity (kN/m^2); G is shear elastic constant (kN/m^2); A is sectional size (m^2); c_p is pressure wave damping constant; c_s is shear wave damping constant.

$$\lambda = \frac{\mu E}{(1+\mu)(1-2\mu)};$$
$$G = \frac{E}{2(1+\mu)}. \quad (6)$$

In the formula, μ is Poisson's ratio; E is elastic coefficient (kN/m^2).

The damping constant is listed in Table 4.

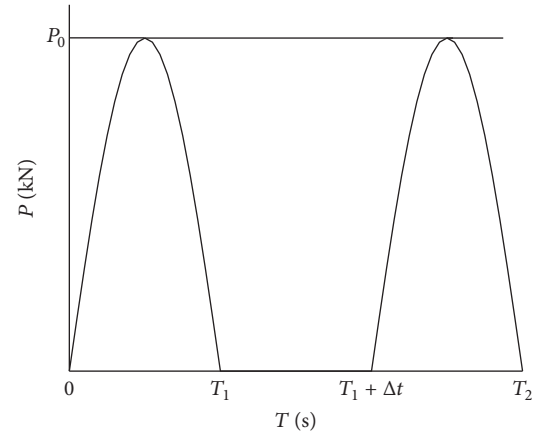

Figure 5: Sine motor vehicle load curve oscillogram.

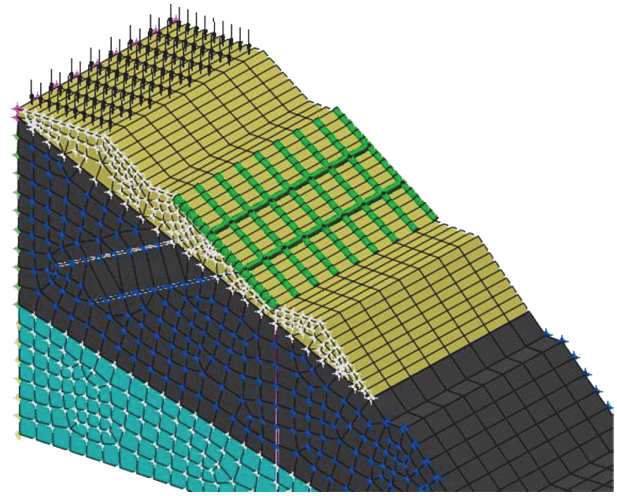

Figure 6: Sine motor vehicle load curve oscillogram.

4.2. Slope Time-Histories Analysis under Sinusoidal Dynamic Load. To get the relevant mass and stiffness coefficient, the immediate integration is utilized to analyze the linear time-histories, using the result of eigenvalue period put into damping ratio calculation function.

According to the domestic and overseas research on vehicle dynamic load [16], the pressure induced by the process of cars moving can be approximately simulated by the repeated and discontinuous sine wave. Based on the ⟨Code for design of highway subgrades⟩ JTGD30-2004 and the site conditions about road reconstruction and its traffic service [17], the load is set to 50 kN/m. Furthermore, it is modeled to sine wave, determining that the maximum concentrated force on the rebuild road is 500 kN.

In Figure 5, T is the time of wheel acting on the road; Δt is headway time; P_0 is the amplitude of peak load. And sine motor vehicle load curve oscillogram is shown in Figure 6.

4.3. Time-Histories Displacement Analysis. Under the vehicle load, the bedding slope displacement fringes at horizontal and vertical direction are shown in the following, respectively.

Table 4: Damping constant of every stratum.

Damping constant kN·s/m	Intermediate weathered sandstone kN/m^3	Intermediate weathered silty mudstone kN/m^3	Strong weathered silty mudstone kN/m^3
P	3565.91	2815.85	247.31
S	2248.48	1531.40	142.78

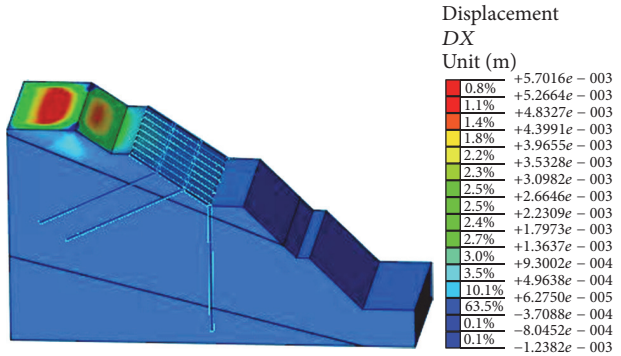

Figure 7: Sine load horizontal displacement analysis cloud picture.

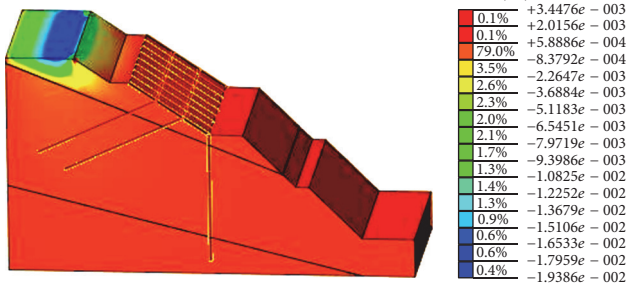

Figure 8: Sine load vertical displacement analysis cloud picture.

According to Figures 7 and 8, under sine wave load, displacement response at rebuilt road occurs at both vertical and horizontal direction. However, the displacement does not enlarge enough to form a continuous connecting slip surface, insuring the slope stable. To be more specific, the displacement at two directions is small, which includes horizontal 5.29 mm and vertical 18.71 mm.

As shown in Figure 9, five characteristic nodes are chosen at the horizontal symmetric axes, and Figures 10 and 11 illustrate the horizontal displacement and settlement of the five nodes under sine wave vehicle load.

As shown in Figure 10, under the sine wave load, the displacement response rule of every node is the same; in addition, Node A has the most obvious response with the maximum amplitude 5.29 mm.

According to Figure 11, under the sine wave vehicle load, the settlements at 5 nodes are almost the same. Yet, Node C has the largest settlement value at 18.71 mm, which is different from horizontal displacement.

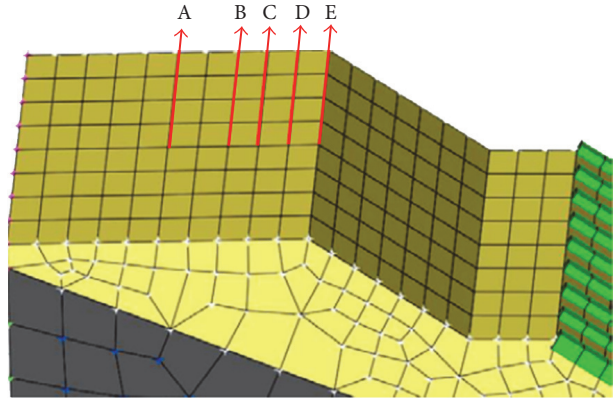

Figure 9: Characteristics point schematic diagram.

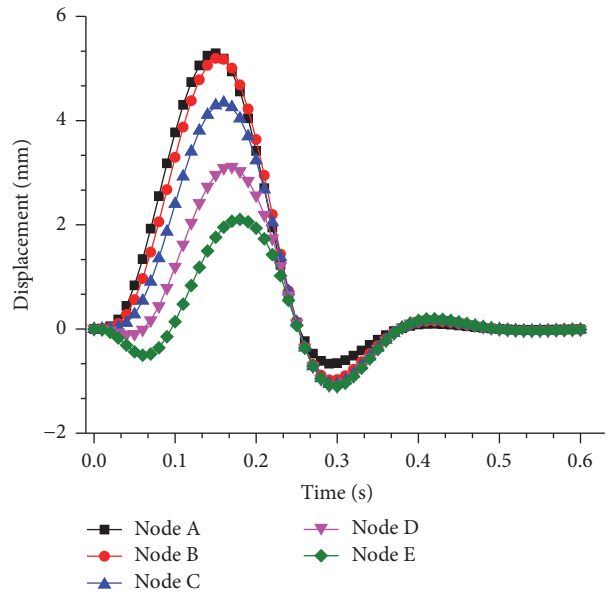

Figure 10: Slope time-history analysis horizontal displacement curve.

Moreover, when using beam element to simulate the slide-resistant pile, thrust value at axis of slide-resistant pile can be obtained directly, by calculating the difference force value in front of and behind the pile [18]. The cross section of slope, under sine wave load, and bearing the most stress are chosen and analyzed, getting the horizontal internal force figure of response effectiveness as shown in Figures 12 and 13.

Figure 12 has shown that, under sine wave load, antislide force of pile shows the same response rule in line with slope horizontal displacement. At the initial stage, internal force

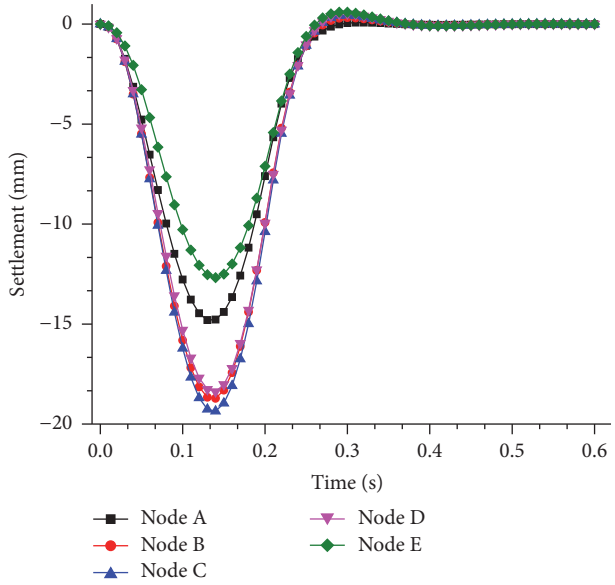

Figure 11: Slope time-history analysis settlement displacement curve.

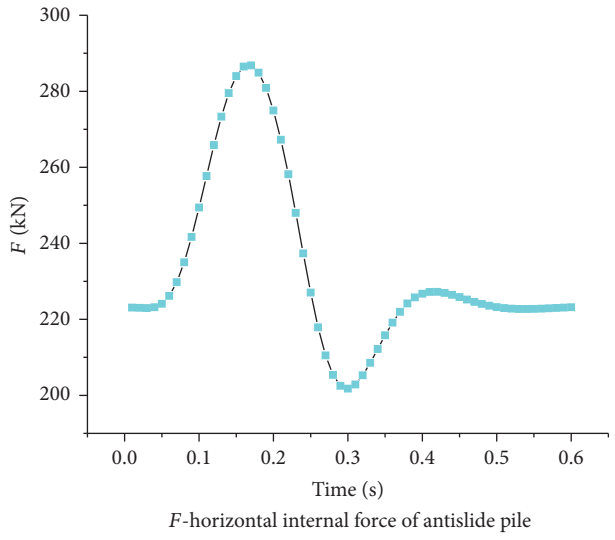

Figure 12: Antisliding internal force response effect curve.

in the pile induced by load changes little; primarily it is influenced by the acting position and magnitude of load. As the displacement transmits to the slope toe, the antislide pile plays more and more significant part in offering resistance, showing more obvious dynamic response. The maximum internal force acting on pile is 286.80 kN at horizontal direction, while the minimum is 201.78 kN.

Figure 13 illustrates that under the specific load, the sensitivity of prestressed anchor cable is better than antislide pile, because of the acting position and load magnitude. Internal force of anchor cable is 180.69 kN at most and 95.68 kN at least.

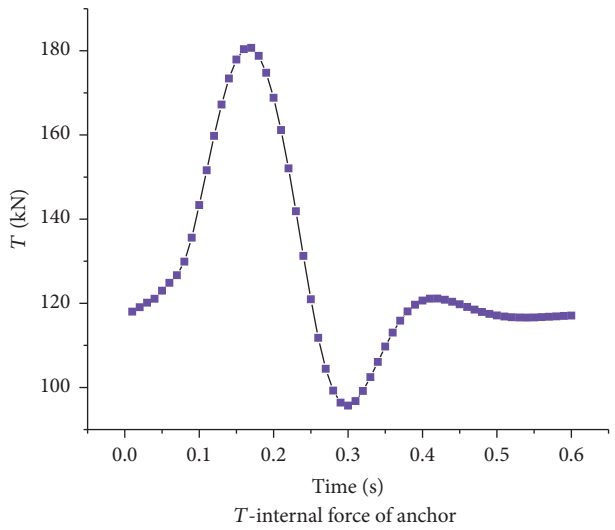

Figure 13: Anchor cable internal force response effect curve.

Figure 14: Anchor cable stress tester.

5. Synergism Analysis of Piles and Anchor Cable Support

Under specific dynamic load, the range of maximum and minimum internal force value in the slope with piles and anchor cable support or antislide pile is named reasonable coordinate interval. According to the real-time monitoring data of slope, the internal force of anchor or antislide pile is within the reasonable coordinate interval, which means that the slope is safe; yet, if the force is out of it, that means overload causes compressive stress redistribution, furthermore, increasing the possibility of landslide, which must be brought to the forefront.

The slope on right side of express highway under construction in Fuling-Fengdu-Shizhu, Chongqing section of K27+140~27+380, is set as the instance [19], monitoring the internal force borne by piles and anchor cable support in the slope, using anchor cable stress tester to test the internal force of anchor cable and using soil pressure gauge to test the internal force of antislide pile. Figure 14 shows using the anchor cable stress tester to test the internal force of anchor cable. Moreover, Figure 16 shows using the soil pressure box to test internal force of antislide pile.

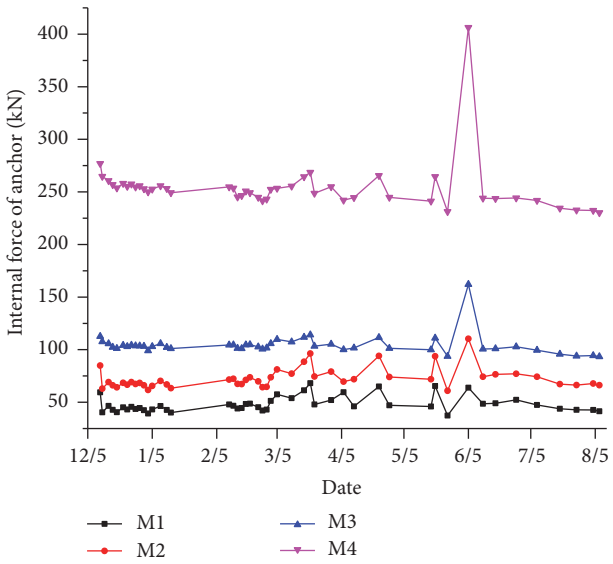

Figure 15: Anchor internal force with time variation curve.

Figure 16: Soil pressure gauge.

The internal force curves of anchor and antislide pile are shown in Figures 15 and 17.

On one hand, the antislide pile internal force at horizontal direction can be calculated through the value obtained by the anchor stress detector. On the other hand, the cross section bearing the largest internal force is monitored and calculated with integration and then it is concluded that the internal force in the horizontal direction of the anchor pile is 115.92 kN and the horizontal direction of the antislide pile is 225.64 kN.

Based on the concept of reasonable coordinate interval, the anchor interval is [95.68, 180.69], and the pile is [201.78, 286.80]. According to the field monitoring data, the internal force of the anchor (115.92 kN) and the antislide pile (225.64 kN) is in the reasonable range, which means that the slope is at steady state under the sine wave vehicle load.

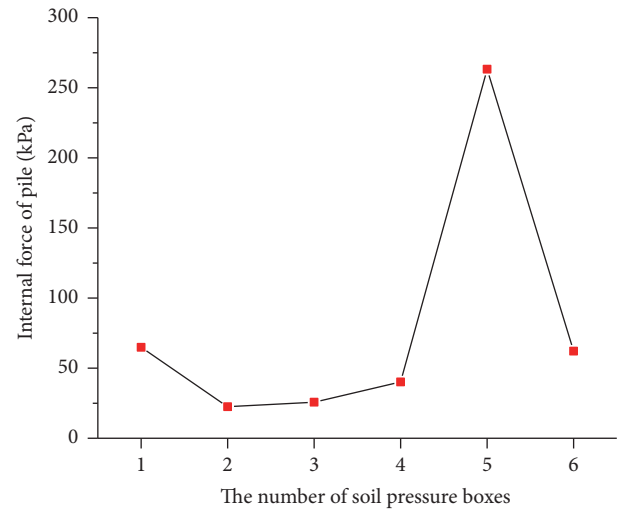

Figure 17: Antislide pile internal force curve.

6. Conclusion

Based on the simulation of sine wave vehicle load acting on the bedding slope, the surface viscous boundary proposed by Lysmer and conventional ground support boundary are united to calculate the eigenvalue and time-histories, reaching the dynamic response of anchor pile composite structure, proposing the conception of reasonable coordinate interval under dynamic load. The conclusion is as follows:

(1) Under the dynamic load, both anchor and pile can bear the sliding force; furthermore, they coordinate.

(2) The sensitivity of responding the dynamic load in the structure anchor and pile is different, which is related to the load position and magnitude.

(3) Proposing the conception of reasonable coordinate, it is verified by evaluating the slope stability in engineering project.

In this paper, the concept of coordinated interval can be used to evaluate the stability of dynamic loads and a new method to control dynamic load on slope.

Competing Interests

The authors declare that they have no competing interests.

References

[1] J. H. Dong and Y. P. Zhu, "Calculation method of soil nailed slope stability under seismic action," *Journal of Vibration and Shock*, vol. 28, no. 3, pp. 119–124, 2009.

[2] J. Z. Le, H. Z. Qiu, and L. J. Zhang, "Analysis on dynamic response of the foundation pit supporting structure under traffic loads," *Chinese Journal of Underground Space and Engineering*, vol. 9, no. 6, pp. 1320–1325, 2013.

[3] Y. Luo, S.-M. He, C.-J. Ouyang, and Y. Wu, "Stability analysis of pile and anchor composite structure reinforced slope under

the earthquake loading," *Sichuan Daxue Xuebao (Engineering Science Edition)*, vol. 42, no. 1, pp. 93–99, 2010.

[4] H.-X. Guo, E.-X. Song, and Z.-Y. Chen, "Excavation influential surface of soil nailing and its application in estimating the nail tensile forces," *Engineering Mechanics*, vol. 24, no. 11, pp. 82–87, 2007.

[5] Z. D. Zhu, J. X. Hao, and L. M. Zhao, "Deformation characteristics of silt subgrade under traffic loads," *Chinese Journal of Underground Space and Engineering*, vol. 5, no. 5, pp. 1013–1019, 2009.

[6] L. G. Fang, Z. B. Sun, and Q. Wang, "The analysis of mechanism and stability of slope reinforced with the pre-forced cable and anti-slipping pile," *Highway Engineering*, vol. 32, no. 4, pp. 152–155, 2007.

[7] Y. Luo, Q. Xu, S.-M. He, and J.-C. He, "Stability analysis of slopes reinforced with gravity walls under the earthquake loading," *Engineering Mechanics*, vol. 30, no. 9, pp. 132–138, 2013.

[8] X. Weng, J. Chen, and J. Wang, "Fiber Bragg grating-based performance monitoring of piles fiber in a geotechnical centrifugal model test," *Advances in Materials Science and Engineering*, vol. 2014, Article ID 659276, 8 pages, 2014.

[9] R. D. Hryciw, "Anchor design for slope stabilization by surface loading," *Journal of Geotechnical Engineering*, vol. 117, no. 8, pp. 1260–1274, 1991.

[10] G.-D. Zhang, F. Chen, X. Jin, Y. Li, and R.-B. Li, "Effect of different boundary conditions and seismic waves on seismic response of a slope," *Journal of Vibration and Shock*, vol. 30, no. 1, pp. 102–105, 2011.

[11] I. Baron, V. Cilek, O. Krejci, R. Melichar, and F. Hubatka, "Structure and dynamics of deep-seated slope failures in the Magura Flysch Nappe, outer Western Carpathians (Czech Republic)," *Natural Hazards and Earth System Science*, vol. 4, no. 4, pp. 549–562, 2004.

[12] F. Agliardi, G. Crosta, and A. Zanchi, "Structural constraints on deep-seated slope deformation kinematics," *Engineering Geology*, vol. 59, no. 1-2, pp. 83–102, 2001.

[13] C. Sagaseta, J. M. Sánchez, and J. Cañizal, "A general analytical solution for the required anchor force in rock slopes with toppling failure," *International Journal of Rock Mechanics and Mining Sciences*, vol. 38, no. 3, pp. 421–435, 2001.

[14] H. T. Wang, *MIDAS/GTS Numerical Analysis in Geotechnical Engineering and Design*, vol. 9, Dalian University of Technology Press, 2013.

[15] G. Y. Liao and X. M. Huang, *ABAQUS Application of Finite Element Software in Highway Engineering*, Southeast University Press, 2008.

[16] M. Hyodo and K. Yasuhara, "Analytical procedure for evaluating pore-water pressure and deformation of saturated clay ground subjected to traffic loads," in *Proceedings of the 6th International Conference on Numerical Methods in Geomechanics*, vol. 1, pp. 653–658, Innsbruck, Austria, April 1988.

[17] S. W. Liu, J. Zhang, and S. Ling, "Study on dynamic behavior of asymmetric reinforced embankment under traffic load," *Journal of Zhengzhou University: Engineering Science*, vol. 2, pp. 41–45, 2014.

[18] Y. R. Zheng, S. Y. Zhao, A. H. Li et al., *FEM Limit Analysis and Its Application in Slope Engineering*, China Communications Press, Beijing, China, 2011.

[19] D. F. Li, L. J. Wang, B. J. Ge, and T. Shan, "Anti-slide analysis on the combination structure of anchor framework beam and pile in high slope sliding along lightly inclined strata," *Journal of Beijing Jiaotong University*, vol. 38, no. 4, pp. 137–142, 2014.